

ANALYSIS OF NOZZLE DESIGN USED FOR THE CREATION OF ADVANCED ENERGY BEAM

Nan Yu¹, Renaud Jourdain¹, Mustapha Gourma², Paul Shore^{1,3}

¹Precision Engineering Institute, Cranfield University

²Department of Engineering Computing, Cranfield University

³Loxham Precision Limited

Bedfordshire, England, UK

INTRODUCTION

A variety of scientific and industrial projects, such as segmented ground based telescopes, compact space based observers, short wavelength microlithography and high power laser systems, demand metre scale ultra-precise surfaces [1]. Cranfield University and Loxham Precision have been engaged in developing effective fabrication of medium to large optical surfaces for the aforementioned applications. A process chain of three sequential machining steps has been proposed (Figure 1). These steps are ultra-precision grinding, robot based polishing and plasma figuring. The fabrication target is to reach a 20 hours cycle time for each stage of surface generation for 1.5m size optics: equating to 1ft² per hour [2-3].

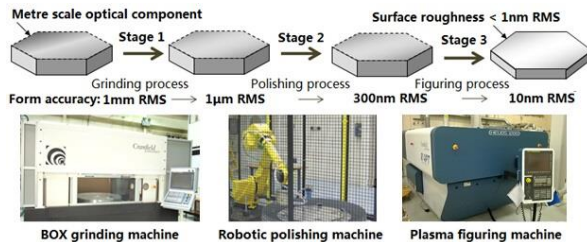


FIGURE 1. Proposed rapid production line for large scale mirror segment fabrication [2].

BACKGROUND

The final processing step of this fabrication chain is a state-of-the-art plasma figuring process. This figuring process uses an Inductively Coupled Plasma (ICP) torch whose motion is managed by the dwell time algorithm that provides a controllable chemical reaction for etching local regions of a surface. The use of an ICP torch for the study of surface aberrations was carried at Lawrence Livermore National Laboratory (LLNL) in the late 1990s by Dr Jeffrey Carr et al [4-7]. From this work a series of processing systems were created. The measurement of the plasma temperature has been carried out by Dr William O'Brien [8]. The

largest and most sophisticated plasma figuring machine was created in 2008 through a collaboration between RAPT Industries of the US and Cranfield University in England. The so-called Helios 1200 is a unique 1.2 metre scale plasma surface figuring facility housed within the Cranfield University Precision Engineering Institute [9]. In 2012, Castelli et al [10] demonstrated fast figure correction of near meter scale optical surfaces to 30nm RMS form accuracy using this plasma technology.

This large scale plasma facility uses an ICP torch which is operated at atmospheric pressure. The plasma torch is able to create a highly collimated plasma beam, in which fluorine atoms are introduced. These fluorine atoms react with silicon-based substrates. Typically, material removal rate of $\sim 1.5 \text{ mm}^3/\text{min}$ is achieved. The material removal footprint the ICP torch is characterised by a Gaussian cross sectional having "soft edges". An important feature of the plasma torch is its dedicated nozzle. This nozzle is mounted onto the end of the ICP torch. The nozzle design determines the size, shape and plasma velocity of the energy beam as it impinges the processed surfaces.

The processing of metre scale optical surfaces achieved in 2012 was successful both in terms of processing duration and form accuracy. Plasma figuring of a 440mm sized substrate was performed in less than 2.5 hours achieving 30nm RMS form accuracy from an initial 2.5 micrometre PV value. However, mid spatial frequency (MSF) structure was evident [11-12]. This surface structure was assessed and linked to the raster-scanning parameters and ICP torch nozzle design. Figure 2 highlights this surface structure showing the main spatial frequency and its harmonics.

The identified and undesired residual surface features need to be removed. To accomplish

this improvement, the use of smaller scale energy beams has been suggested [12]. The energy beam footprint achieved in the previous research is shown in Figure 3. It can be seen that Full Width at Half Maximum (FWHM) is 12mm.

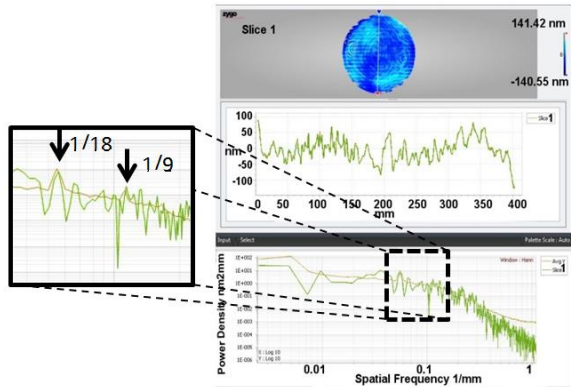


FIGURE 2. Surface structure showing MSF features [11-12]. (In 2012, Jourdain and Castelli scrutinised the MSF on a 400mm diameter surface processed by plasma figuring process)

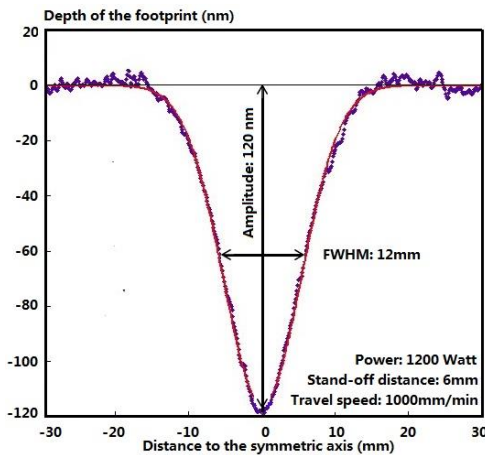


FIGURE 3. Footprint of the trench (cross section)

Numerical simulation of the plasma torch nozzle is considered essential to investigate and understand the physical and chemical processes taking place. Previously, Professor Boulos and Professor Proulx have created computational fluid dynamics (CFD) models for subsonic and supersonic ICP torch systems [13-16]. The fluid description of the plasma was based on the Navier-Stokes conservation equations for mass, momentum and energy. Many properties of the plasma and its behaviours in the ICP torch have been investigated through those models.

The purpose of the work presented in this paper is to advance the plasma figuring of optical surfaces through the development of optimised ICP torches and associated nozzles. This research aims at providing highly collimated energy beams characterized by a material removal footprint of between 1mm and 5mm FWHM.

This paper describes initial work towards the creation of a CFD model of the plasma process with initial attempts to correlate the CFD results with plasma beam removal footprint data. This CFD model work is developed to help establish the important design rules for new nozzles.

NUMERICAL SIMULATION OF PLASMA NOZZLE DESIGNS

This paper introduces initial CFD modelling of the plasma torch nozzle designs. As a first study the CFD model evaluates the aerodynamics of the gas flow. A number of assumptions are made regarding the fluid. The fluid is considered to be high temperature argon gas, it is also assumed axisymmetric, uniform, steady and laminar. Consequently, a simple 2D cross-sectional model of De-Laval nozzle design has been created. This model is based in the software package FLUENT (Figure 4).

The CFD model boundary conditions include: flow input velocity, gas type, gas temperature, and pressure distribution. The initial entry temperature is set at 6000 Kelvin as supported by the PhD work of Dr O'Brien.

Figure 4 shows a 3D drawing of the ICP torch and a cross-section of the current nozzle as modelled in the FLUENT software. Argon is fed into the nozzle through the upper aperture and flows downward in an axis-symmetric manner. Two areas are of interest in this work: the De-Laval throat and the near surface substrate region where the chemical reaction takes place. This second area is the focus of this paper.

To ease explanation a line of study is defined at 10 μm from the substrates surface. This line is entitled the "Pathway of Investigation", see Figure 4.

As shown in Figure 5 the "Pathway of Investigation" is characterised by regions experiencing either downwards and upwards flow directions. The regions experiencing downwards flow are shown with a negative

value in Figure 5. Regions along the Pathway of Investigation that experiences an upwards vertical flow component are shown having a positive value.

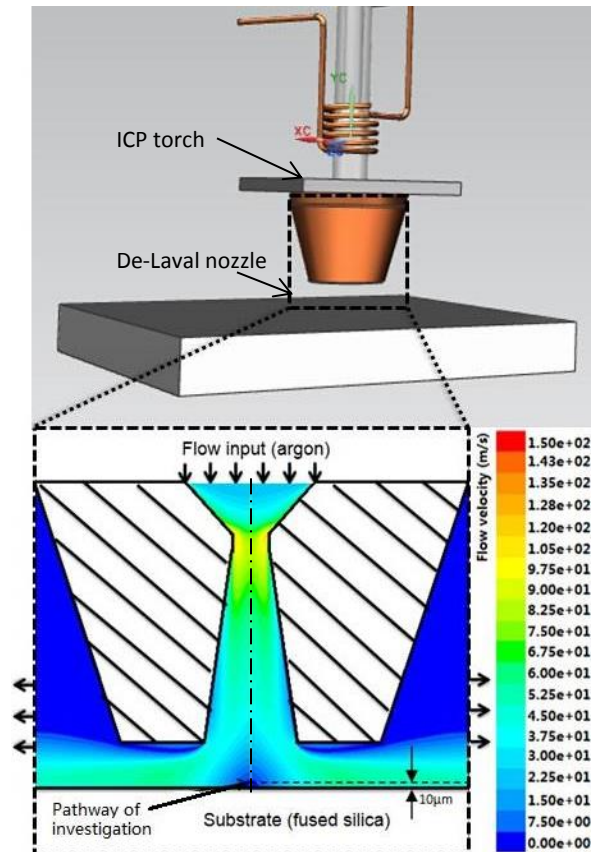


FIGURE 4. Overview of the CFD investigation. 3D drawing of the plasma figuring torch (upper); 2D CFD simulation illustration of flow velocity in the nozzle (lower).

The negative regions are considered to be those which will experience the presence of the radical compounds. The CFD model is able to determine the amplitude and direction of these particles and consequently help understand the regions of preferential etching.

From a processing view point, the plasma etching is considered to take place only in the region exposed to free radicals, because the fluorine radicals in the plasma jet can be in contact with the silicon atoms of the substrate. This assumption is supported by experimental tests performed by Dr Fanara. In the future this assumption will be further validated through tests using differing nozzle designs. However, there seems to be good initial indications supporting this assumption from footprint

experiments carried out at Cranfield in 2010 by Dr Castelli. The 4 sigma value of the footprint - 22 mm (11mm radius) is very close to the 10.5 mm radius exposed to free radicals as shown in Figure 5.

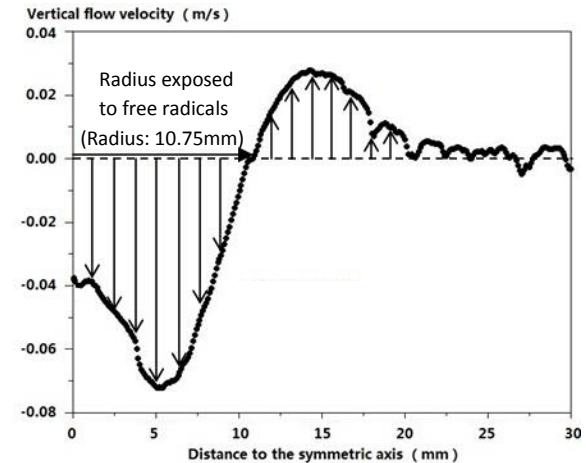


FIGURE 5. Vertical flow velocity plots along the pathway of investigation.

Figure 6 combines images from the gas flow simulation and footprint experiment. This figure enables to highlight the correlation between the material removal footprint and the regions along the "Pathway on Investigation" that experiences a downwards vertical flow profile.

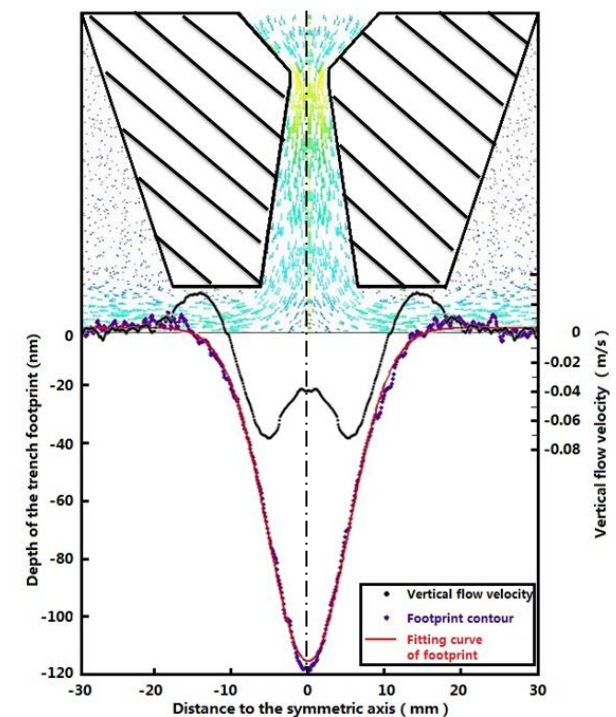


FIGURE 6. Curves of the etched area and gas velocity.

In Figure 6, the black curve shows the amplitude of the vertical velocity of the gas along the near surface regions of the substrate, whilst the blue plot shows the actual footprint removal profile obtained by Dr Castelli.

NOZZLE DESIGN EVALUATION USING CFD MODEL

Investigation of the nozzle's key design parameters based on the aforementioned 2D axis-symmetric numerical model has been made. Evaluation is based on the changing radius along the Pathway of Investigation that is exposed to free radicals. The hydrodynamic characteristics of the De-Laval nozzle depend on seven parameters (shown in Table 1). Three of them have been changed to investigate their effect on gas flow. The three design parameters varied were: the diameter of the throat D_2 , the diameter of divergent end D_3 , and the depth of the divergent path h_3 . The following paragraphs detail the findings and results obtained through the CFD model focussing on the radius exposed to free radicals and the maximum velocity in the throat.

Effect of the Throat Diameter

The throat-parameter D_2 - in the De-Laval nozzle is crucial, because the speed of flow increases strongly when the gas goes through this narrow section. A five-step increase of the throat diameter (4.0mm, 4.3mm, 4.7mm, 5.0mm and 5.3mm) is chosen for the investigation of the flow velocity change. The correlation between the diameter of the throat and the radius exposed to free radicals is highlighted in Figure 7. When D_2 decreases by 24%, the radius exposed to free radicals decreases by 19%. The sensitivity of D_2 is 0.79. Also it can be

observed that the flow velocity increases when the throat dimension gets smaller.

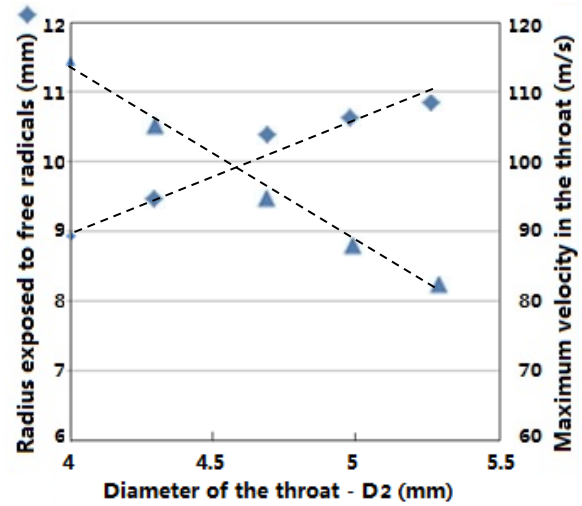


FIGURE 7. The throat diameter (D_2) versus the radius exposed to free radicals (\blacklozenge left), and D_2 versus the maximum velocity in the throat (\blacktriangle right).

Effect of the Divergent End Dimension

Similar comparison is made among nozzles with different dimensions of divergent end diameter - parameter D_3 -. The chosen diameters are 10.8mm, 11.4mm, 12.0mm, 12.6mm, 13.2mm and 16.7mm. The correlation between the diameter of the divergent end and the radius exposed to free radicals can be seen in Figure 8. As expected, the results show that a wider divergent end generates a larger etched area. The dimension of the etched area decreases 8% as D_3 shrinks 18%. The sensitivity of D_3 is 0.44. The maximum flow velocity through the throat is little affected by this nozzle parameter.

TABLE 1. Parameters of the nozzle in the characteristic analysis.

No	Parameters	Symbol	Schematic plot
1	Diameter of convergent end	D_1	
2	Diameter of throat	D_2	
3	Diameter of divergent end	D_3	
4	Depth of convergent path	h_1	
5	Depth of throat	h_2	
6	Depth of divergent path	h_3	
7	Stand-off distance	h_4	

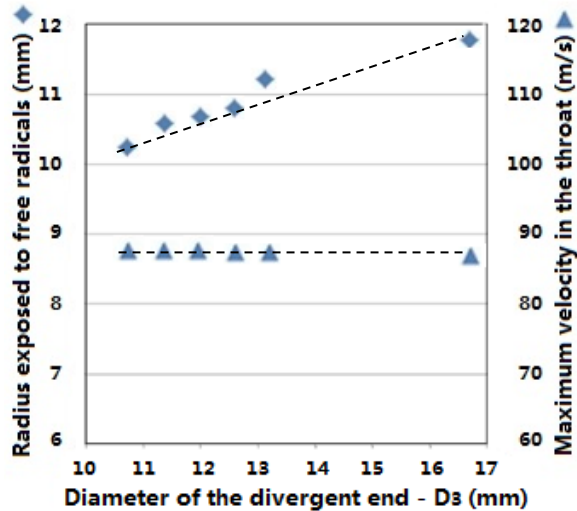


FIGURE 8. The divergent end dimensions (D_3) versus the radius exposed to free radicals (\blacklozenge left), and D_3 versus the maximum velocity in the throat (\blacktriangle right).

Effect of the Divergent Path Dimension

Through this third investigation, the influence of the dimension of the divergent path - parameter h_3 - is analysed. Here two scenarios are investigated.

First scenario: the diameter of the divergent end is kept constant at 11.4mm. Thus the change of divergence path dimension affects the divergent angle which consequently increases. Unlike the last two comparisons, the obvious change of the divergent depth doesn't change the radius exposed to free radicals (Figure 9).

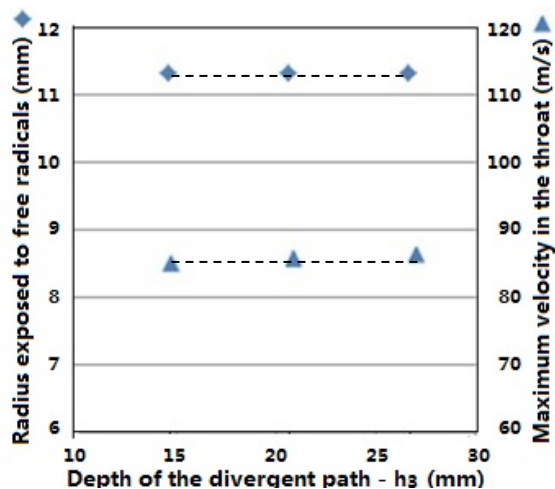


FIGURE 9. The depth of the divergent path (h_3) versus the radius exposed to free radicals (\blacklozenge left), and h_3 versus the maximum velocity in the throat (\blacktriangle right). (Divergent angle changes with h_3)

Second scenario: the angle of divergence is kept constant and therefore the divergent path dimension is altered. It can be seen in Figure 10 that the short nozzle reduces the radius exposed to free radicals. However, the response from h_3 is not obvious comparing to that of D_2 and D_3 .

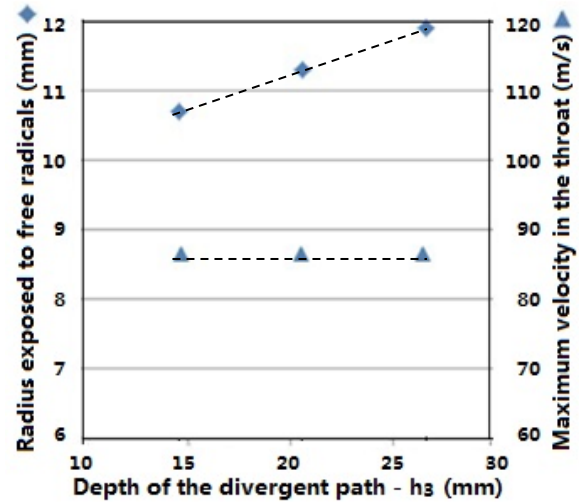


FIGURE 10. The depth of the divergent path (h_3) versus the radius exposed to free radicals (\blacklozenge left), and h_3 versus the maximum velocity in the throat (\blacktriangle right). (Divergent angle is kept constant)

These last two sets of results are complementary and they enable to correlate the radius exposed to free radicals and the diameter of the divergent end. Moreover, from the series of results obtained through this initial modelling work, there are three general design rules of the De-Laval nozzle:

1. Radius exposed to free radicals decreases significantly as the throat (D_2) shrinks;
2. Radius exposed to free radicals decreases when the divergent end (D_3) shrinks.
3. Smaller energy beam footprints should be achieved with adjustment of D_2 as it is more efficient than tuning D_3 .

CONCLUSIONS

A 2D axis-symmetry numerical model of an existing torch nozzle has been created. This initial model has indicated some sensible results when compared to actual process data of removal footprints. Initial correlation data gives confidence for more detailed modelling work.

Some initial design rules and nozzle parameter sensitivity analysis has been obtained. This

information can be used to create a number of new nozzle designs for future experiments.

Limitations of this CFD model include the use of argon flow instead of a plasma flow and insufficient supporting experimental data. These limitations will be addressed by the lead author during the next 2 years of his PhD.

FUTURE WORK

The CFD model will be advanced by:

1. Measurement using plasma diagnostic for more accurate parameters including initial entry flow velocity and temperature, heat loss in the nozzle;
2. Definition for the ionization and recombination of the argon particle and its electron so as to simulate argon plasma instead of pure argon;
3. Taking the turbulence and swirl into account;
4. Further validation through material removal footprint trials using differing nozzle designs.

Using the developed CFD model new nozzles and torch designs will be created. These new torch / nozzle designs will be employed to establish an effective plasma process that rapidly removes MSF for large scale metre class optics.

ACKNOWLEDGEMENT

This research work was funded by the Centre for Innovative Manufacturing in Ultra Precision of the Engineering and Physical Sciences Research Council (EPSRC) UK.

REFERENCES

- [1] Shore P, Morantz P, Read R, Tonnellier X, Comley P, Jourdain R, Castelli M. Productive Modes for Ultra-Precision Grinding of Freeform Optics. ASPE, Kohala Coast, Hawaii, USA. 26th-27th June, 2014.
- [2] Shore P, Cunningham C, DeBra D, Evans D, Hough J, Gilmozzi R, Kunzmann H, Morantz P, Tonnellier X. Precision engineering for astronomy and gravity science. CIRP Annals – Manufacturing Technology. 2010; 59: 694–716.
- [3] Shore P. Ultra precision surfaces. Proceeding of ASPE, Portland, Oregon, USA. 2008; 75-78.
- [4] Carr, J.W., RAPT Industries Inc. Apparatus and method for reactive atom plasma processing for material deposition. 2011, US Patent, 7955513 B2.

- [5] Carr, J.W., RAPT Industries Inc. Method for atmospheric pressure reactive atom plasma processing for surface modification. 2009, US Patent, 7591957 B2.
- [6] Chang A, Carr J.W., Kelley J, Fiske P.S., RAPT Industries Inc. Systems and methods utilizing an aperture with a reactive atom plasma torch. 2007, US Patent, 7304263 B2.
- [7] Carr J, Atmospheric Pressure Plasma Processing for Damage - Free Optics and Surfaces. Engineering research Development and Technology. 1999; 3: 31-39.
- [8] O'Brien W. Characterisation and Material Removal Properties of the RAPTM Process (PhD thesis), Cranfield University, Cranfield, UK: 2011.
- [9] Jourdain R, Castelli M, Shore P, Sommer P, Proscia D. Reactive atom plasma (RAP) figuring machine for meter class optical surfaces. Production Engineering Research & Development. 2013; 6: 665-673.
- [10] Castelli M, Jourdain R, Morantz P, Shore P. Rapid optical surface figuring using reactive atom plasma. Precision Engineering. 2012; 36: 467-476.
- [11] Jourdain R, Castelli M, Morantz P, Shore P. Plasma Surface Figuring of Large Optical Components. SPIE, Photonics Europe, Belgium, 16th-19th April, 2012.
- [12] Castelli M. Advances in Optical Surface Figuring by Reactive Atom Plasma (RAP) (PhD thesis), Cranfield University, Cranfield, UK: 2013.
- [13] Morsli EI, Proulx P. A chemical non-equilibrium model of an air supersonic ICP. Journal of Physics D: Applied Physics, 2007, 40: 308-394.
- [14] Murphy A.B., Boulous M.I., Colombo V, et al. Advanced thermal plasma modelling. High Temperature Material Processes (An International Quarterly of High-Technology Plasma Processes), 2008, 12(3-4).
- [15] Morsli EI, Proulx P. Two-temperature chemically non-equilibrium modelling of an air supersonic ICP. Journal of Physics D: Applied Physics, 2007, 40(16): 4810.
- [16] Boulous M.I., Jurewicz J.W., Tekna Plasma Systems Inc. Process and apparatus for the manufacture of a sputtering target. 2011, US Patent, 7964247 B2.